



MOX-Report No. 20/2023

**A multigrid method for PDE-constrained optimization with uncertain
inputs**

Ciaramella, G.; Nobile, F.; Vanzan, T.

MOX, Dipartimento di Matematica
Politecnico di Milano, Via Bonardi 9 - 20133 Milano (Italy)

mox-dmat@polimi.it

<https://mox.polimi.it>

and \mathcal{R} is a risk measure. The vectors $\{\mathbf{y}_j\}_{j=1}^N$ and $\{\mathbf{p}_j\}_{j=1}^N$ are the discretizations of the state and adjoint variables $y(\omega)$ and $p(\omega)$ at the N samples in which the random PDE constraint is collocated. The vector \mathbf{u} is the discretization of the deterministic control u . Problems of the form (1.3) are increasingly employed in applications. The PDE constraints typically represent some underlying physical model whose behaviour should be optimally controlled, and the randomness in the PDE allows one to take into account the intrinsic variability or lack of knowledge on some parameters entering the model. The introduction of a risk measure in (1.3) allows one to construct robust controls that take into account the distribution of the cost over all possible realizations of the random parameters. Therefore, the topic has received a lot of attention in the last years, see, e.g. [19, 20, 28, 16, 15, 1, 30, 13, 2].

However, few works have focused on efficient solvers for the optimality systems (1.1). A popular approach is to perform a Schur complement on \mathbf{u} and solve the reduced system with a Krylov method (possibly with Conjugate Gradient), despite each iteration would then require the solution of $2N$ PDEs, with A_j and A_j^\top for $j = 1, \dots, N$ [18]. For a full-space formulation, block diagonal preconditioners have been studied in [29], using both an algebraic approach based on Schur complement approximations, and an operator preconditioning framework.

In this manuscript, we present a multigrid method to solve general problems of the form (1.1) and show how this strategy can be used for the efficient solution of three different Optimal Control Problems Under Uncertainty (OCPUU). First, we consider a linear-quadratic OCPUU and use the multigrid algorithm directly to solve the linear optimality system. Second, we consider a nonsmooth OCPUU with box constraints and L^1 regularization on the control. To solve such problem, we use the collective multigrid method as an inner solver within an outer semismooth Newton iteration. Incidentally, we show that the theory developed for the deterministic OCPs with L^1 regularization can be naturally extended to the class of OCPUU considered here. Third, we study a risk-adverse OCPUU involving the smoothed Conditional Value at Risk (CVaR) and test the performance of the multigrid scheme in the context of a nonlinear preconditioned Newton method.

The multigrid algorithm is based on a collective smoother [5, 6, 38] that, at each iteration, loops over all nodes of the computational mesh (possibly in parallel), collects all the degrees of freedom related to a node, and updates them collectively by solving a reduced saddle-point problem. For classical (deterministic) PDE-constrained optimization problems, this reduced system has size 3×3 so that its solution is immediate [6]. In our context, the reduced problem has size $(2N + 1) \times (2N + 1)$, so that it can be large when dealing with a large number of samples. Fortunately, we show that it can be solved with optimal $O(N)$ complexity. Let us remark that collective multigrid strategies have been applied to OCPUU in [7, 4] and in [34]. This manuscript differs from the mentioned works since, on the one hand, [7, 4] considers a *stochastic* control u , therefore for (almost) every realization of the random parameters a different control $u(\omega)$ is computed through the solution of a standard deterministic OCP. On the other hand, [34] considers a Stochastic Galerkin discretization, and hence the corresponding optimality system has a structure which is very different from (1.2).

The multigrid algorithm assumes that all variables are discretized on the same finite element mesh. Further, despite we here consider only the case of a global distributed control, the smoothing procedure could be extended to a local distributed control on a subset \tilde{D} of the computational domain \mathcal{D} , and to boundary control, see,

e.g., [5].

The rest of the manuscript is organized as follows. In Section 2 we introduce the notation, a classical linear-quadratic OCPUU, and interpret (1.2) as the matrix associated to an optimality system of the discretized OCPUU. In Section 3, we present the collective multigrid algorithm, discuss implementation details and show its performance to solve the linear-quadratic OCPUU. In Section 4, we consider a nonsmooth OCPUU with box constraints and a L^1 regularization on the control. Section 5 deals with a risk-adverse OCPUU. For each of these cases, we first show how the multigrid approach can be integrated in the solution process, by detailing concrete algorithms, and then we present extensive numerical experiments to show the efficiency of the proposed framework. Finally, we draw our conclusions in Section 6.

2. A linear-quadratic optimal control problem under uncertainty. Let \mathcal{D} be a Lipschitz bounded domain in \mathbb{R}^d , V the standard Sobolev space $H_0^1(D)$, and $(\Omega, \mathcal{F}, \mathbb{P})$ a complete probability space.

Given a function $u \in L^2(\mathcal{D})$, we consider the linear elliptic random PDE

$$(2.1) \quad a_\omega(y, v) = (u, v), \forall v \in V, \quad \mathbb{P}\text{-a.e. } \omega \in \Omega,$$

where (\cdot, \cdot) denotes the standard $L^2(\mathcal{D})$ scalar product. To assure uniqueness and sufficient integrability of the solution of (2.1), we make the following additional assumption.

Assumption 2.1. There exist two random variables $a_{\min}(\omega)$ and $a_{\max}(\omega)$ such that

$$a_{\min}(\omega) \|v\|_V^2 \leq a_\omega(v, v) \leq a_{\max}(\omega) \|v\|_V^2, \quad \forall v \in V, \quad \mathbb{P}\text{-a.e. } \omega \in \Omega,$$

and further a_{\min} and a_{\max} are in $L^p(\Omega)$ for some $p \geq 4$.

Under Assumption 2.1, it is well-known (see, e.g., [25, 10]) that (2.1) admits a solution in V for \mathbb{P} -a.e. ω , and the solution y , interpreted as a function-valued random variable $y : \omega \in \Omega \mapsto y(\omega) \in V$, lies in the Bochner space $L^p(\Omega; V)$ [12]. We often use the shorthand notation $y_\omega = y(x, \omega)$ when the dependence on x is not needed, or $y_\omega(u)$ when we want to highlight the dependence on the control function u .

In this manuscript, we consider the minimization of functionals constrained by (2.1). Let us first focus on the linear-quadratic problem

$$(2.2) \quad \min_{u \in L^2(\mathcal{D})} \frac{1}{2} \mathbb{E} \left[\|y_\omega - y_d\|_{L^2(\mathcal{D})}^2 \right] + \frac{\nu}{2} \|u\|_{L^2(\mathcal{D})}^2,$$

where $y_\omega \in V$ solves

$$a_\omega(y_\omega, v) = (u + f, v), \quad \forall v \in V, \quad \mathbb{P}\text{-a.e. } \omega \in \Omega,$$

where $y_d \in L^2(\mathcal{D})$ is a target state, $f \in L^2(\mathcal{D})$ (we omit the continuous embedding operators from $L^2(\mathcal{D})$ to $L^2(\Omega; L^2(\mathcal{D}))$), $\mathbb{E} : L^1(\Omega) \rightarrow \mathbb{R}$ is the expectation operator and $\nu > 0$. Introducing the linear control-to-state map $S : u \in L^2(\mathcal{D}) \rightarrow y_\omega(u) \in L^2(\Omega; L^2(\mathcal{D}))$, we reformulate (2.2) as,

$$(2.3) \quad \min_{u \in L^2(\mathcal{D})} \frac{1}{2} \mathbb{E} \left[\|S(u) - y_d\|_{L^2(\mathcal{D})}^2 \right] + \frac{\nu}{2} \|u\|_{L^2(\mathcal{D})}^2.$$

Existence and uniqueness of the minimizer of (2.3) follows directly from standard variational arguments [24, 17, 39, 19]. Furthermore, due to Assumption 2.1, the optimal control \bar{u} satisfies the variational equality

$$(2.4) \quad (\nu \bar{u} - S^*(y_d - S(\bar{u} + f)), v)_{L^2(\mathcal{D})} = 0, \quad \forall v \in L^2(\mathcal{D}),$$

where the adjoint operator $S^* : L^2(\Omega; L^2(\mathcal{D})) \rightarrow L^2(\mathcal{D})$, satisfying $(Su, z)_{L^2(\Omega; L^2(\mathcal{D}))} = (u, S^*z)_{L^2(\mathcal{D})}$, is characterized by $S^*z = \mathbb{E}[p]$ where $p = p_\omega(x)$ is the solution of the adjoint equation

$$(2.5) \quad a_\omega(v, p_\omega) = (z(\omega), v), \quad \forall v \in V, \quad \mathbb{P}\text{-a.e. } \omega \in \Omega.$$

The optimality condition (2.4) can thus be formulated as the optimality system

$$(2.6) \quad \begin{aligned} a_\omega(y_\omega, v) &= (\bar{u} + f, v), \quad \forall v \in V, \quad \mathbb{P}\text{-a.e. } \omega \in \Omega, \\ a_\omega(v, p_\omega) &= (y_d - y_\omega, v), \quad \forall v \in V, \quad \mathbb{P}\text{-a.e. } \omega \in \Omega, \\ (\nu \bar{u} - \mathbb{E}[p_\omega], v)_{L^2(\mathcal{D})} &= 0, \quad \forall v \in L^2(\mathcal{D}). \end{aligned}$$

To solve numerically (2.2), we replace the exact expectation operator \mathbb{E} of the objective functional by a quadrature formula $\widehat{\mathbb{E}}$ with N nodes $\{\omega_i\}_{i=1}^N$ and positive weights $\{\zeta_i\}_{i=1}^N$, namely

$$\mathbb{E}[X] \approx \widehat{\mathbb{E}}[X] := \sum_{i=1}^N \zeta_i X(\omega_i), \quad \text{with} \quad \sum_{i=1}^N \zeta_i = 1.$$

Common quadrature formulae are Monte Carlo, Quasi-Monte Carlo and Gaussian formulae. The latter requires that the probability space can be parametrized by a sequence (finite or countable) of random variables $\{\chi_j\}_j$, each with distribution μ_j , and the existence of a complete basis of tensorized $L^2_{\mu_j}$ -orthonormal polynomials. Hence for the semi-discrete OCP, the \mathbb{P} -a.e. PDE-constraint is naturally collocated onto the nodes of the quadrature formula.

Concerning the space domain, we consider a family of regular triangulations $\{\mathcal{T}_h\}_{h>0}$ of \mathcal{D} , and a Galerkin projection onto the finite element space V^h of continuous piecewise polynomial functions of degree r over \mathcal{T}_h that vanish on $\partial\mathcal{D}$, spanned by a Lagrangian basis. N_h is the dimension of V^h , and $\{\phi\}_{i=1}^{N_h}$ is a nodal Lagrangian basis. We discretize the state, adjoint and control variables on the same finite element space.

Once fully discretized, (2.6) can be expressed as

$$(2.7) \quad \begin{pmatrix} M_s & & & & & & A_1^\top \\ & \ddots & & & & & \ddots \\ & & M_s & & & & A_N^\top \\ & & & \nu M_s & -w_1 M_s & \dots & -w_N M_s \\ A_1 & & & -M_s & & & \\ & \ddots & & \vdots & & & \\ & & A_N & -M_s & & & \end{pmatrix} \begin{pmatrix} \mathbf{y}_1 \\ \vdots \\ \mathbf{y}_N \\ \mathbf{u} \\ \mathbf{p}_1 \\ \vdots \\ \mathbf{p}_N \end{pmatrix} = \begin{pmatrix} M_s \mathbf{y}_d \\ \vdots \\ M_s \mathbf{y}_d \\ \mathbf{0} \\ M_s \mathbf{f} \\ \vdots \\ M_s \mathbf{f} \end{pmatrix},$$

where A_j are the stiffness matrices associated to the bilinear forms $a_{\omega_j}(\cdot, \cdot)$, M_s is the mass matrix, \mathbf{y}_d and \mathbf{f} are the finite element discretizations of y_d and f respectively, while \mathbf{y}_j and \mathbf{p}_j are the discretizations of y_{ω_j} and p_{ω_j} .

3. Collective multigrid scheme. In this section, we describe the multigrid algorithm to solve the full space optimality system (2.7). For the sake of generality, we consider the more general matrix (1.2), so that our discussion covers also the different saddle-point matrices obtained in Sections 4 and 5.

For each node of the triangulation, let us introduce the vectors $\tilde{\mathbf{y}}_i$ and $\tilde{\mathbf{p}}_i$,

$$\tilde{\mathbf{y}}_i = \begin{pmatrix} (\mathbf{y}_1)_i \\ \vdots \\ (\mathbf{y}_N)_i \end{pmatrix} \in \mathbb{R}^N, \quad \tilde{\mathbf{p}}_i = \begin{pmatrix} (\mathbf{p}_1)_i \\ \vdots \\ (\mathbf{p}_N)_i \end{pmatrix} \in \mathbb{R}^N, \quad i = 1, \dots, N_h,$$

which collect the degrees of freedom associated to the i -th node, the scalar $u_i = (\mathbf{u})_i$, and the restriction operators $R_i \in \mathbb{R}^{(2N+1)N_h \times 2N+1}$ such that

$$R_i \begin{pmatrix} \mathbf{y} \\ \mathbf{u} \\ \mathbf{p} \end{pmatrix} = \begin{pmatrix} \tilde{\mathbf{y}}_i \\ u_i \\ \tilde{\mathbf{p}}_i \end{pmatrix} =: \mathbf{x}_i.$$

The prolongation operators are $P_i := R_i^\top$, while the reduced matrices $\tilde{S}_i := R_i S P_i \in \mathbb{R}^{2N+1 \times 2N+1}$ represent a condensed saddle-point matrix on the i -th node, and satisfy

$$(3.1) \quad \tilde{S}_i = \begin{pmatrix} \text{diag}(\mathbf{c}_i) & 0 & \text{diag}(\mathbf{a}_i) \\ 0 & (G)_{i,i} & \mathbf{d}_i^\top \\ \text{diag}(\mathbf{a}_i) & \mathbf{e}_i & 0 \end{pmatrix}$$

with $\mathbf{c}_i := ((C_1)_{i,i}, \dots, (C_N)_{i,i})^\top$, $\mathbf{a}_i := ((A_1)_{i,i}, \dots, (A_N)_{i,i})^\top$, $\mathbf{e}_i := ((E_1)_{i,i}, \dots, (E_N)_{i,i})^\top$, $\mathbf{d}_i := ((D_1)_{i,i}, \dots, (D_N)_{i,i})$, where $\text{diag}(\mathbf{v})$ denotes a diagonal matrix with the components of \mathbf{v} on the main diagonal.

Given an initial vector \mathbf{x}^0 , a Jacobi-type collective smoothing iteration computes for $n = 1, \dots, n_1$,

$$(3.2) \quad \mathbf{x}^n = (1 - \theta)\mathbf{x}^{n-1} + \theta \sum_{i=1}^{N_h} P_i \tilde{S}_i^{-1} R_i (\mathbf{f} - S\mathbf{x}^{n-1}),$$

where $\theta \in (0, 1]$ is a damping parameter. Gauss-Seidel variants can straightforwardly be defined. Next, we consider a sequence of meshes $\{\mathcal{T}_{h_\ell}\}_{\ell=\ell_{\min}}^{\ell_{\max}}$, which we assume for simplicity to be nested, and restriction and prolongator operators $R_{\ell-1}^\ell, P_{\ell-1}^\ell$ which map between grids $\mathcal{T}_{h_{\ell-1}}$ and \mathcal{T}_{h_ℓ} . In the numerical experiments, the coarse matrices are defined recursively in a Galerkin fashion starting from the finest one, namely $S_\ell := R_\ell^{\ell+1} S_{\ell+1} P_\ell^{\ell+1}$ for $\ell \in \{1, \dots, \ell_{\max} - 1\}$. Nevertheless it is obviously possible to define S_ℓ as the discretization of the continuous saddle-point system onto the mesh \mathcal{T}_{h_ℓ} . With this notation, the V-cycle collective multigrid is described by Algorithm 3.1, which can be repeated until a certain stopping criterium is satisfied. We used the notation *Collective_Smoothing*(\cdot, \cdot, \cdot) to denote possible variants of (3.2) (e.g. Gauss-Seidel).

Notice that (3.2) requires to invert the matrices S_i for each computational node. We now show that this can be done with optimal $O(N)$ complexity. Indeed, performing a Schur complement on u_i , the system $\tilde{S}_i \mathbf{x}_i = \mathbf{f}_i$, with $\mathbf{f}_i = (\mathbf{f}_{p_i}, b_{u_i}, \mathbf{f}_{y_i})^\top$ can be solved exclusively computing inverses of diagonal matrices and scalar products between vectors through

$$(3.3) \quad \begin{aligned} u_i &= \frac{b_{u_i} + \mathbf{d}_i^\top (\text{diag}(\mathbf{a}_i)^{-1} \text{diag}(\mathbf{c}_i) \text{diag}(\mathbf{a}_i)^{-1} \mathbf{f}_{y_i} - \text{diag}(\mathbf{a}_i)^{-1} \mathbf{f}_{p_i})}{(G)_{i,i} + \mathbf{d}_i^\top \text{diag}(\mathbf{a}_i)^{-1} \text{diag}(\mathbf{c}_i) \text{diag}(\mathbf{a}_i)^{-1} \mathbf{e}_i}, \\ \tilde{\mathbf{y}}_i &= (\text{diag}(\mathbf{a}_i))^{-1} (\mathbf{f}_{y_i} - \mathbf{e}_i u_i), \\ \tilde{\mathbf{p}}_i &= (\text{diag}(\mathbf{a}_i))^{-1} (\mathbf{f}_{p_i} - \text{diag}(\mathbf{c}_i) \tilde{\mathbf{y}}_i). \end{aligned}$$

Algorithm 3.1 V-cycle Collective Multigrid Algorithm - V-cycle($\mathbf{x}^0, \mathbf{f}, \ell$)

```

1: if  $\ell = \ell_{\min}$ , then
2:   set  $\mathbf{x}^0 = S_{\ell_{\min}}^{-1} \mathbf{f}$ .                (direct solver)
3: else
4:    $\mathbf{x}^{n_1} = \text{Collective\_Smoothing}(\mathbf{x}^0, S_\ell, n_1)$   ( $n_1$  steps of collective smoothing)
5:    $\mathbf{r} = \mathbf{f} - S_\ell \mathbf{x}^{n_1}$                         (compute the residual)
6:    $\mathbf{e}_c = \text{V-cycle}(\mathbf{0}, R_{\ell-1}^\ell \mathbf{r}, \ell - 1)$ .      (recursive call)
7:    $\mathbf{x}^0 = \mathbf{x}^{n_1} + P_{\ell-1}^\ell \mathbf{e}_c$                 (coarse correction)
8:    $\mathbf{x}^{n_2} = \text{Collective\_Smoothing}(\mathbf{x}^0, S_\ell, n_2)$  ( $n_2$  steps of collective smoothing)
9:   Set  $\mathbf{x}^0 = \mathbf{x}^{n_2}$                             (update)
10: end if
11: return  $\mathbf{x}^0$ .

```

Notice that we should guarantee that $\text{diag}(\mathbf{a}_i)$ admits an inverse and that $(G)_{i,i} + \mathbf{d}_i^\top \text{diag}(\mathbf{a}_i)^{-1} \text{diag}(\mathbf{c}_i) \text{diag}(\mathbf{a}_i)^{-1} \mathbf{e}_i \neq 0$. This has to be verified case by case, so we now focus on the specific matrix (2.7). On the one hand, the vectors \mathbf{a}_i are strictly positive componentwise, since $(\mathbf{a}_i)_j = a_{\omega_j}(\phi_i, \phi_i) > 0 \forall i = 1, \dots, N_h, j = 1, \dots, N$ (due to Assumption 2.1). On the other hand, $(G)_{i,i} = \int_{\mathcal{D}} \phi_i^2(x) dx > 0$, while a direct calculation shows that

$$\mathbf{d}_i^\top \text{diag}(\mathbf{a}_i)^{-1} \text{diag}(\mathbf{c}_i) \text{diag}(\mathbf{a}_i)^{-1} \mathbf{e}_i = (M_s)_{i,i}^3 \sum_{j=1}^N w_j (A_j)_{i,i}^{-2} > 0,$$

which implies that (3.3) is well-defined.

Assuming that the V-cycle algorithm requires a constant number of iterations to reach a given tolerance as both N_h, N and the number of levels increase (so that the size of the coarse problem becomes negligible in the limit), Algorithm 3.1 exhibits an overall optimal linear complexity $O(N_h N)$ since asymptotically the cost of each iteration is dominated by the N_h relaxation steps, each of a cost proportional to N due to the above discussion. In the next numerical experiments sections, we show indeed that the number of iterations remain constant for several test cases.

3.1. Numerical experiments. We now show the performance of Alg. 3.1 and its robustness with respect to several parameters for the solution of (2.7). We consider the state equation

$$(3.4) \quad a_\omega(y_\omega, v) = \int_D \kappa(x, \omega) \nabla y(x, \omega) \cdot \nabla v(x) dx = \int_{\mathcal{D}} u(x) v(x) dx, \quad \forall v \in V, \mathbb{P}\text{-a.e. } \omega \in \Omega,$$

in a domain $\mathcal{D} = (0, 1)^2$ discretized with a regular mesh of squares of edge $h_\ell = 2^{-\ell}$, which are then decomposed into two right triangles. We choose $\kappa(x, \omega)$ as an approximated log-normal diffusion field

$$(3.5) \quad \kappa(x, \omega) = e^{\sigma \sum_{j=1}^M \sqrt{\lambda_j} b_j(x) N_j(\omega)} \approx e^{g(x, \omega)},$$

where $g(x, \omega)$ is a mean zero Gaussian field with Covariance function $\text{Cov}_g(x, y) = \sigma^2 e^{-\frac{\|x-y\|_2^2}{L^2}}$. The parameter σ^2 tunes the variance of the random field, while L denotes the correlation length. The pairs $(b_j(x), \sigma^2 \lambda_j)$ are the eigenpairs of $T : L^2(\mathcal{D}) \rightarrow L^2(\mathcal{D})$, $(Tf)(x) = \int_{\mathcal{D}} \text{Cov}_g(x, y) f(y) dy$, and $N_j \sim \mathcal{N}(0, 1)$. Assumption 2.1 is satisfied since $a_{\min}(\omega) = (\text{ess inf}_{x \in \mathcal{D}} \kappa(x, \omega))^{-1}$ and $a_{\max}(\omega) = \|\kappa(\cdot, \omega)\|_{L^\infty(\mathcal{D})}$ are in $L^p(\Omega)$

for every $p < \infty$ [9]. We first consider $L^2 = 0.5$, so that setting $M = 3$ into (3.5) is enough to keep 99% of the variance, and we discretize the problem using the Stochastic Collocation method [3] on Gauss-Hermite tensorized quadrature nodes. The target state is $y_d = e^{y^2} \sin(2\pi x) \sin(2\pi y)$.

Table 1 shows the number of V-cycle iterations (Alg. 3.1) and of GMRES iterations preconditioned by the V-cycle (in brackets) to solve (2.7) up to a tolerance of 10^{-9} on the relative (unpreconditioned) residual. Inside the V-cycle algorithm, we use $n_1 = n_2 = 2$ pre- and post-smoothing iterations based on the Jacobi relaxation (3.2) with a damping parameter $\theta = 0.5$. The number of levels of the V-cycle hierarchy is denoted with N_L .

TABLE 1

Number of V-cycle iterations and preconditioned GMRES iterations (in brackets) to solve (2.7).

| | | | | |
|-------|-----------|-----------|-----------|-----------|
| ν | 10^{-2} | 10^{-4} | 10^{-6} | 10^{-8} |
| It. | 17 (11) | 19 (13) | 19 (15) | 19 (14) |

$N_h = 961, N = 125, N_L = 3, \sigma^2 = 0.5, L^2 = 0.5.$

| | | | | |
|------------|---------|---------|---------|---------|
| σ^2 | 0.1 | 0.5 | 1 | 1.5 |
| It. | 19 (12) | 19 (13) | 19 (13) | 19 (14) |

$N_h = 961, N = 125, N_L = 3, \nu = 10^{-4}, L^2 = 0.5.$

| | | | |
|------------|---------|---------|----------|
| $N_h(N_L)$ | 225 (2) | 961 (3) | 3969 (4) |
| It. | 18 (13) | 19 (13) | 19 (13) |

$N = 125, \nu = 10^{-4}, \sigma^2 = 0.5, L^2 = 0.5.$

| | | | | |
|-----|---------|---------|---------|---------|
| N | 8 | 27 | 64 | 125 |
| It. | 19 (12) | 19 (12) | 19 (13) | 19 (13) |

$N_h = 961, \nu = 10^{-4}, \sigma^2 = 0.5, L^2 = 0.5.$

The multigrid algorithm has a perfect robustness with respect to all parameters considered. In particular, the convergence does not deteriorate as $\nu \rightarrow 0$, which is a well-known troublesome limit for several preconditioners (see, e.g., [29, 32, 31, 11] and references therein). Further, the third sub-table shows the robustness of the algorithm with respect to the number of levels as the fine grid is refined. The fourth sub-table instead shows that the number of iteration remains constant as the discretization of the probability space is refined. As a complementary experiment, we next consider $L^2 = 0.025$ and use a Monte Carlo quadrature formula, since Stochastic Collocation suffers from the curse of dimensionality. We also refine the spatial grid to properly capture the variations of the random diffusion coefficient. Table 2 confirms the robustness of the algorithm even for much larger numbers of samples.

4. An optimal control problem under uncertainty with box-constraints and L^1 penalization. In this section, we consider the nonsmooth OCPUU

$$(4.1) \quad \min_{u \in U_{ad}} \frac{1}{2} \mathbb{E} \left[\|y_\omega(u) - y_d\|_{L^2(\mathcal{D})}^2 \right] + \frac{\nu}{2} \|u\|_{L^2(\mathcal{D})}^2 + \beta \|u\|_{L^1(\mathcal{D})},$$

where $y_\omega(u) \in V$ solves

$$a_\omega(y_\omega(u), v) = (u + f, v), \quad \forall v \in V, \quad \mathbb{P}\text{-a.e. } \omega \in \Omega,$$

$$U_{ad} := \{v \in L^2(\mathcal{D}) : a \leq u \leq b \text{ almost everywhere in } \mathcal{D}\},$$

TABLE 2

Number of V-cycle iterations and preconditioned GMRES iterations (in brackets) to solve (2.7).

| | | |
|-----|---------|---------|
| N | 100 | 1000 |
| It. | 21 (14) | 21 (14) |

$$N_h = 3969, \nu = 10^{-4}, N_L = 3, \sigma^2 = 1.5, L^2 = 0.025.$$

with $a < 0 < b$ and $\nu, \beta > 0$. Deterministic OCPs with a L^1 penalization lead to optimal controls which are sparse, i.e. they are nonzero only on certain regions of the domain \mathcal{D} [37, 8]. Sparse controls can be of great interest in applications, because it is often not desirable, or even impossible, to control the system over the whole domain \mathcal{D} . For sparse OCPUU, we mention [23] where the authors considered both a simplified version of (4.1) in which the randomness enters linearly into the state equation as a force term, and a different optimization problem whose goal is to find a stochastic control $u(\omega)$ which has a similar sparsity pattern regardless of the realization ω . Notice further that the assumption $\nu > 0$ does not eliminate the nonsmoothness of the objective functional, but it regularizes the optimal solution u , and is needed to use the fast optimization algorithm described in the following.

The well-posedness of (4.1) follows directly from standard variational arguments [39, 17], being U_{ad} a convex set, $\varphi(u) := \beta \|u\|_{L^1(\mathcal{D})}$ a convex function and the objective functional coercive. In particular, the optimal solution \bar{u} satisfies the variational inequality ([14, Proposition 2.2])

$$(4.2) \quad (\nu \bar{u} - S^*(y_d - S(\bar{u} + f)), \bar{u} - v) + \varphi(\bar{u}) - \varphi(v) \geq 0, \quad \forall v \in U_{ad}.$$

Through a pointwise discussion of the box constraints and an analysis of a Lagrange multiplier belonging to the subdifferential of φ in \bar{u} , [37] showed that (4.2) can be equivalently formulated as the nonlinear equation $\mathcal{F}(\bar{u}) = 0$, with $\mathcal{F} : L^2(\mathcal{D}) \rightarrow L^2(\mathcal{D})$ defined as

$$(4.3) \quad \mathcal{F}(u) := u - \frac{1}{\nu} (\max(0, \mathcal{T}u - \beta) + \min(0, \mathcal{T}u + \beta) - \max(0, \mathcal{T}u - \beta - \nu b) - \min(0, \mathcal{T}u + \beta - \nu a)),$$

where $\mathcal{T} : L^2(\mathcal{D}) \ni u \rightarrow -S^*(Su) + S^*(y_d - Sf) \in L^2(\mathcal{D})$. Notice that \mathcal{F} is nonsmooth due to the presence of the Lipschitz functions $\max(\cdot)$ and $\min(\cdot)$. Nevertheless, \mathcal{F} can be shown to be semismooth [17], provided that \mathcal{T} is continuously Fréchet differentiable, and further Lipschitz continuous interpreted as map from $\mathcal{T} : L^2(\mathcal{D}) \rightarrow L^r(\mathcal{D})$, with $r > 2$ [40, 17]. These conditions are satisfied also in our settings since \mathcal{T} is affine and further the adjoint variable p_ω , solution of (2.5) with $z = y_d - S(u + f)$, lies in $L^2(\Omega, H_0^1(\mathcal{D}))$ so that $\mathcal{T}u = \mathbb{E}[p_\omega] \in H_0^1(\mathcal{D}) \subset L^r(\mathcal{D})$, where $r > 2$ follows from the Sobolev embeddings.

Hence, to solve (4.3) we use the semismooth Newton method whose iteration reads for $k = 1, 2, \dots$ until convergence,

$$(4.4) \quad u^{k+1} = u^k + du^k, \quad \text{with } \mathcal{G}(u^k)du^k = -\mathcal{F}(u^k),$$

$\mathcal{G}(u) : L^2(\mathcal{D}) \rightarrow L^2(\mathcal{D})$ being the generalized derivative of \mathcal{F} . Using the linearity of \mathcal{T} and considering the supports of the weak derivatives of $\max(0, x)$ and $\min(0, x)$, we obtain that

$$(4.5) \quad \mathcal{G}(u)[v] = v + \frac{1}{\nu} \chi_{(I^+ \cup I^-)} S^* S v,$$

Algorithm 4.1 Globalized semismooth Newton Algorithm to solve $\mathbf{F}(\mathbf{u}) = 0$

Require: \mathbf{u}^0 , $\text{Tol} \in \mathbb{R}^+$, $\sigma, \rho \in (0, 1)$.

- 1: $\mathbf{y}_j^0 = A_j^{-1}(M_s(\mathbf{f} + \mathbf{u}^0))$, $\mathbf{p}_j^0 = (A_j^\top)^{-1}(M_s(\mathbf{y}_d - \mathbf{y}_j^0))$, $j = 1, \dots, N$.
Set $k = 0$ and define I_0^+ and I_0^- using (4.9).
 - 2: **while** $\phi(\mathbf{u}^k) > \text{Tol}$ **do**
 - 3: Solve (4.8) calling Alg. 3.1 until convergence.
 - 4: Set $\gamma = 1$
 - 5: **while** $\phi(\mathbf{u}^k + \gamma \mathbf{d}\mathbf{u}^k) - \phi(\mathbf{u}^k) > -\sigma\phi(\mathbf{u}^k)$ **do**
 - 6: $\gamma = \rho\gamma$.
 - 7: **end while**
 - 8: Update $\mathbf{u}^{k+1} = \mathbf{u}^k + \gamma \mathbf{d}\mathbf{u}^k$, $\mathbf{y}_j^{k+1} = \mathbf{y}_j^k + \gamma \mathbf{d}\mathbf{y}_j^k$, $\mathbf{p}_j^{k+1} = \mathbf{p}_j^k + \gamma \mathbf{d}\mathbf{p}_j^k$, $j = 1, \dots, N$.
 - 9: Update I_k^+ and I_k^- using (4.9).
 - 10: Set $k = k + 1$.
 - 11: **end while**
 - 12: **return** \mathbf{u}^k , \mathbf{y}_j^k and \mathbf{p}_j^k , $j = 1, \dots, N$.
-

use the collective multigrid algorithm to solve it. Further, with the notation of (1.2), it holds

$$(G)_{i,i} + d_i^\top \text{diag}(a_i)^{-1} \text{diag}(c_i) \text{diag}(a_i)^{-1} e_i = (M_s)_{i,i} + (M_s)_{i,i}^3 \sum_{j=1}^N w_j (A_j)_{i,i}^{-2} > 0$$

if $i \in I^+ \cup I^-$, and

$$(G)_{i,i} + d_i^\top \text{diag}(a_i)^{-1} \text{diag}(c_i) \text{diag}(a_i)^{-1} e_i = (M_s)_{i,i} > 0,$$

if $i \notin I^+ \cup I^-$. The collective multigrid iteration is then well-defined.

The overall semismooth Newton Algorithm is summarized in Algorithm 4.1. At each iteration we solve (4.8) using the collective multigrid algorithm (line 3) and update the active sets given the new iteration (line 9). Notice that in order to globalize the convergence, we consider a line-search step (lines 5-7) performed on the merit function $\phi(\mathbf{u}) = \sqrt{\mathbf{F}(\mathbf{u})^\top M_s \mathbf{F}(\mathbf{u})}$ [27].

4.1. Numerical experiments. In this section we test the semismooth Newton algorithm for the solution of (4.3) and the collective multigrid algorithm to solve the related optimality system (4.8). We consider the random PDE-constraint (3.4) with the random diffusion coefficient (3.5). The semismooth iteration is stopped when $\phi(\mathbf{u}^k) < 10^{-9}$. The inner linear solvers are stopped when the relative (unpreconditioned) residual is smaller than 10^{-11} .

Table 3 reports the number of semismooth Newton iterations and in brackets the averaged number of iterations of the V-cycle algorithm used as a solver (left) or as preconditioner for GMRES (right). Table 3 confirms the effectiveness of the multigrid algorithm, which requires essentially the same computational effort than in the linear-quadratic case. Further, except for large values of σ^2 , we numerically observed that the line-search could be omitted without compromising the convergence of the outer iteration.

More challenging is the limit $\nu \rightarrow 0$ reported in Table 4. The performance of both the (globalized) semismooth Newton iteration and the inner multigrid solver

TABLE 3

Number of semismooth Newton iterations, and average number of V-cycle iterations and preconditioned GMRES iterations (in brackets).

| | | | | |
|------------|----------------|---------------|--------------|---------------|
| σ^2 | 0.1 | 0.5 | 1 | 1.5 |
| It. | 3 (22.33-10.3) | 4 (22.5-10.5) | 7(22.8-11.7) | 8 (23.1-11.7) |

$N_h = 961, \nu = 10^{-4}, \beta = 10^{-2}, N = 125, N_L = 3, L^2 = 0.5, b = 50, a = -50.$

| | | | |
|------------|-----------------|---------------|----------------|
| $N_h(N_L)$ | 225 (2) | 961 (3) | 3969 (4) |
| It. | 4 (21.75-11.25) | 4 (22.5-10.5) | 4 (22.5-10.25) |

$\nu = 10^{-4}, \beta = 10^{-2}, N = 125, \sigma^2 = 0.5, L^2 = 0.5, b = 50, a = -50.$

| | | | | |
|-----|------------|---------------|--------------|---------------|
| N | 8 | 27 | 64 | 125 |
| It. | 4 (21-9.7) | 4 (21.5-10.5) | 5 (22.2-9.6) | 4 (22.5-10.5) |

$N_h = 961, \nu = 10^{-4}, \beta = 10^{-2}, \sigma^2 = 0.5, L^2 = 0.5, b = 50, a = -50.$

| | | | | |
|---------|---------------|-----------|-----------|---------------|
| β | 0 | 10^{-4} | 10^{-3} | 10^{-2} |
| It. | 5 (22.2-10.2) | 4 (22-11) | 5 (22-11) | 4 (22.5-10.5) |

$N_h = 961, \nu = 10^{-4}, N = 125, \sigma^2 = 0.5, L^2 = 0.5, b = 50, a = -50.$

TABLE 4

Number of semismooth Newton iterations, and of V-cycle iterations and preconditioned GMRES iterations (in brackets). In the second row, the semismooth Newton method starts from a warm-up initial guess obtained through continuation.

| | | | | |
|-------|------------|---------------|----------------|-----------------|
| ν | 10^{-2} | 10^{-4} | 10^{-6} | 10^{-8} |
| It. | 2 (22-9.5) | 4 (22.5-10.5) | 23 (27.5-12.3) | 52 (45.1-13.7) |
| It. | 2 (22-9.5) | 4 (22-10.5) | 5 (27.6-11.8) | 14 (68.07-17.2) |

$N_h = 961, N = 125, N_L = 3, \sigma^2 = 0.5, L^2 = 0.5, b = 50, a = -50.$

deteriorates. The convergence of the outer nonlinear algorithm can be improved by performing a continuation method, namely we consider a sequence of $\nu = 10^{-j}$, $j = 2, \dots, 8$, and we start the j -th problem using as initial condition the optimal solution computed for $\nu = 10^{-j+1}$. Concerning the inner solver, the stand-alone multigrid algorithm struggles since for small values of ν the optimal control is of bang-bang type, that is satisfies $u = a$, $u = b$ or $u = 0$ for almost every point of the mesh (for $\nu = 10^{-8}$ only seven nodes are nonactive at the optimum). The matrices H^k are then close to zero, and the multigrid hierarchy struggles to capture changes at such small scale. Nevertheless, the multigrid algorithm remains a very efficient preconditioner for GMRES even in this challenging limit.

Fig. 1 shows a sequence of optimal controls for different values of β with and without box-constraints. The optimal control for $\beta = 0$ and without box-constraints corresponds to the minimizer of the linear-quadratic OCP (2.2). We observe that L^1 penalization indeed induces sparsity, since the optimal controls are more and more localized as β increases. Numerically we have verified that for sufficiently large β , the optimal control is identically equal to zero, a property shown in [37].

5. A risk-adverse optimal control problem under uncertainty. In this section we consider an instance of risk-adverse OCPUU. This class of problems has recently drawn lot of attention since in engineering applications it is important to compute a control that minimizes the quantity of interest even in rare, but often

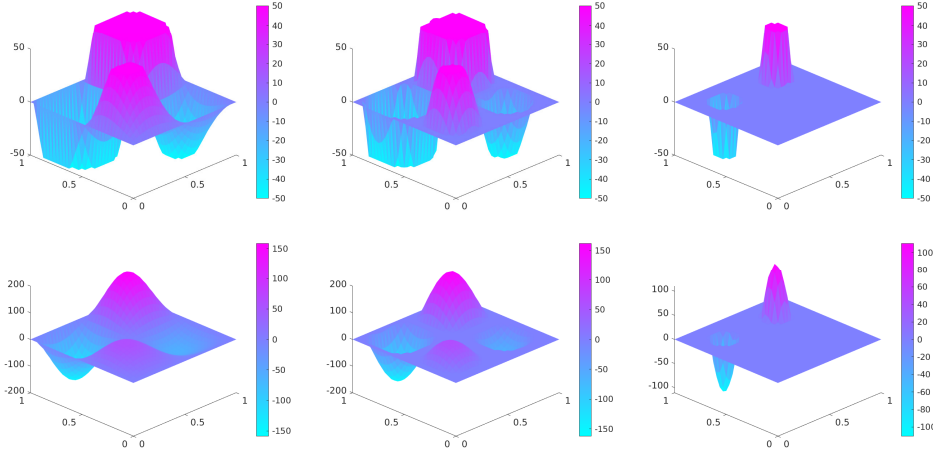


FIG. 1. From left to right: optimal control computed for $\beta \in \{0, 5 \cdot 10^{-3}, 5 \cdot 10^{-2}\}$ with (top row) and without (bottom row) box constraints: $a = -50$, $b = 50$.

troublesome, scenarios [20, 21, 1]. As a risk-measure [35], we use the Conditional Value-At-Risk (CVaR) of confidence level λ , $\lambda \in (0, 1)$,

$$\text{CVaR}_\lambda(X) := \mathbb{E}[X | X \geq \text{VaR}_\lambda(X)], \quad \forall X \in L^1(\Omega; \mathbb{R}),$$

that is, the expected value of a quantity of interest X given that the latter is greater than or equal to its λ -quantile, here denoted by $\text{VaR}_\lambda(X)$. Rockafellar and Uryasev [33] proved that $\text{CVaR}_\lambda(X)$ admits the equivalent formulation

$$(5.1) \quad \text{CVaR}_\lambda(X) = \inf_{t \in \mathbb{R}} \left\{ t + \frac{1}{1-\lambda} \mathbb{E}[(X-t)^+] \right\},$$

where $(\cdot)^+ := \max(0, \cdot)$, if the distribution of X does not have an atom at $\text{VaR}_\lambda(X)$. In order to use tools from smooth optimization, we rely on a smoothing approach proposed in [20], which consists in replacing $(\cdot)^+$ with a smooth function g_ε , $\varepsilon \in \mathbb{R}^+$, such that $g_\varepsilon \rightarrow (\cdot)^+$ in some functional norm as $\varepsilon \rightarrow 0$. Specifically, we choose the C^2 -differentiable approximation

$$(5.2) \quad g_\varepsilon(x) = \begin{cases} 0 & \text{if } x \leq -\frac{\varepsilon}{2}, \\ \frac{(x-\frac{3}{2})^3}{\varepsilon^2} - \frac{(x-\frac{\varepsilon}{2})^4}{2\varepsilon^3} & \text{if } x \in (-\frac{\varepsilon}{2}, \frac{\varepsilon}{2}), \\ x & \text{if } x \geq \frac{\varepsilon}{2}. \end{cases}$$

Then, the smoothed risk-adverse OCPUU is

$$(5.3) \quad \min_{u \in L^2(\mathcal{D}), t \in \mathbb{R}} t + \frac{1}{1-\lambda} \mathbb{E} \left[g_\varepsilon \left(\frac{1}{2} \|y_\omega - y_d\|_{L^2(\mathcal{D})}^2 - t \right) \right] + \frac{\nu}{2} \|u\|_{L^2(\mathcal{D})}^2,$$

where $y_\omega \in V$ solves

$$a_\omega(y_\omega, v) = (u + f, v) \quad \forall v \in V, \mathbb{P}\text{-a.e. } \omega \in \Omega.$$

where $\nu \in \mathbb{R}^+$ and $\lambda \in [0, 1)$. The well-posedness of (5.3), the differentiability of its objective functional, as well as bounds for the error introduced by replacing $(\cdot)^+$ with

$g_\varepsilon(\cdot)$, have been analyzed in [20]. Further, defining $Q_\omega = \frac{1}{2}\|y_\omega - y_d\|_{L^2(\mathcal{D})}^2 - t$, the optimality conditions form the nonlinear system,

$$(5.4) \quad \begin{aligned} a_\omega(v, p_\omega) - \frac{g'_\varepsilon(Q_\omega)}{1-\lambda}(y_d - y_\omega, v) &= 0, & \forall v \in V, \mathbb{P}\text{-a.e. } \omega \in \Omega, \\ (\nu u - \mathbb{E}[p_\omega], v) &= 0, & \forall v \in L^2(\mathcal{D}) \\ a_\omega(y_\omega, v) - (u + f, v) &= 0, & \forall v \in V, \mathbb{P}\text{-a.e. } \omega \in \Omega, \\ 1 - \frac{1}{1-\lambda}\mathbb{E}[g'_\varepsilon(Q_\omega)] &= 0, \end{aligned}$$

Approximating V and \mathbb{E} with V_h and $\widehat{\mathbb{E}}$, and letting $\tilde{\mathbf{x}} = (\mathbf{y}, \mathbf{u}, \mathbf{p}, t)$, the finite-dimensional discretization of (5.4) corresponds to the nonlinear system $\tilde{\mathbf{F}}(\tilde{\mathbf{x}}) = \mathbf{0}$, where $\tilde{\mathbf{F}} : \mathbb{R}^{(2N+1)N_h+1} \rightarrow \mathbb{R}^{(2N+1)N_h+1}$,

$$(5.5) \quad \tilde{\mathbf{F}}(\tilde{\mathbf{x}}) = \begin{pmatrix} \tilde{\mathbf{F}}_1(\tilde{\mathbf{x}}) \\ \tilde{\mathbf{F}}_2(\tilde{\mathbf{x}}) \\ \tilde{\mathbf{F}}_3(\tilde{\mathbf{x}}) \\ \tilde{\mathbf{F}}_4(\tilde{\mathbf{x}}) \end{pmatrix} = \begin{pmatrix} \widetilde{M}(\mathbf{y} - I\mathbf{y}_d) + A^\top \mathbf{p} \\ \nu M_s \mathbf{u} - M_s \widehat{\mathbb{E}}[\mathbf{p}] \\ A\mathbf{y} - M_s(I\mathbf{u} + \mathbf{f}) \\ 1 - \frac{1}{1-\lambda}\widehat{\mathbb{E}}[g'_\varepsilon(Q_\omega)] \end{pmatrix},$$

with $A = \text{diag}(A_1, \dots, A_N)$, $I = [I_{N_h}, \dots, I_{N_h}] \in \mathbb{R}^{N_h \times N_h N}$, I_h being the identity matrix, \mathbf{y}_d is the discretization of y_d , and

$$\widetilde{M} = \text{diag}\left(\frac{g'_\varepsilon(Q_{\omega_1})}{1-\lambda}M_s, \dots, \frac{g'_\varepsilon(Q_{\omega_N})}{1-\lambda}M_s\right), \text{ with } Q_{\omega_j} := \frac{1}{2}(\mathbf{y}_j - \mathbf{y}_d)^\top M_s(\mathbf{y}_j - \mathbf{y}_d) - t,$$

for $j = 1, \dots, N$.

A possible approach to solve (5.5) is to use a Newton method, which given $\mathbf{x}^k = (\mathbf{y}^k, \mathbf{u}^k, \mathbf{p}^k, t^k)$ computes the corrections $\widetilde{\mathbf{d}}\mathbf{x}^k = (\mathbf{d}\mathbf{y}^k, \mathbf{d}\mathbf{u}^k, \mathbf{d}\mathbf{p}^k, dt^k)$ solution of $\tilde{\mathbf{J}}^k \widetilde{\mathbf{d}}\mathbf{x}^k = -\tilde{\mathbf{F}}(\tilde{\mathbf{x}}^k)$, where

$$(5.6) \quad \tilde{\mathbf{J}}^k := \begin{pmatrix} C_1(\mathbf{y}_1^k, t^k) & & & A_1^\top & & & -\mathbf{v}_1^k \\ & \ddots & & & \ddots & & \vdots \\ & & C_N(\mathbf{y}_N^k, t^k) & & & & -\mathbf{v}_N^k \\ & & & \nu M_s & -w_1 M_s & \dots & -w_N M_s \\ A_1 & & & -M_s & & & \\ & \ddots & & \vdots & & & \\ & & A_N & -M_s & & & \\ -w_1 (\mathbf{v}_1^k)^\top & \dots & -w_N (\mathbf{v}_N^k)^\top & & & & \frac{\widehat{\mathbb{E}}[g''_\varepsilon(Q_\omega^k)]}{1-\lambda} \end{pmatrix},$$

with

$$(5.7) \quad Q_{\omega_i}^k := \frac{1}{2}(\mathbf{y}_i^k - \mathbf{y}_d)^\top M_s(\mathbf{y}_i^k - \mathbf{y}_d) - t^k,$$

$$(5.8) \quad C_i(\mathbf{y}_i^k, t^k) := \frac{1}{1-\lambda} (g'_\varepsilon(Q_{\omega_i}^k)M_s + g''_\varepsilon(Q_{\omega_i}^k)M_s(\mathbf{y}_i^k - \mathbf{y}_d)(\mathbf{y}_i^k - \mathbf{y}_d)^\top M_s),$$

$$(5.9) \quad \mathbf{v}_i^k := \frac{1}{1-\lambda} g''_\varepsilon(Q_{\omega_i}^k)M_s(\mathbf{y}_i^k - \mathbf{y}_d),$$

for $i = 1, \dots, N$. Unfortunately, $\tilde{\mathbf{J}}^k$ can be singular away from the optimum, in particular whenever $\widehat{\mathbb{E}}[g''_\varepsilon(Q_\omega^k)] = 0$ which implies

$$(5.10) \quad g''_\varepsilon\left(\frac{1}{2}(\mathbf{y}_j^k - \mathbf{y}_d)^\top M_s(\mathbf{y}_j^k - \mathbf{y}_d) - t^k\right) = 0, \quad \forall j = 1, \dots, N,$$

which is not unlikely for small ε since $\text{supp}(g_\varepsilon'') = (-\frac{\varepsilon}{2}, \frac{\varepsilon}{2})$. Splitting strategies have been proposed (e.g. [26] in a reduced approach), in which whenever (5.10) is satisfied, an intermediate value of t is computed by solving $\tilde{F}_4(t; \mathbf{y}, \mathbf{u}, \mathbf{p}) = 0$ so to violate (5.10). In the next section, we discuss a similar splitting approach. To speed up the convergence of the outer nonlinear algorithm, we use a preconditioned Newton method based on nonlinear elimination [22]. At each iteration we will need to invert saddle-point matrices like (1.2), possibly several times. To do so, we rely on the collective multigrid algorithm.

5.1. Nonlinear preconditioned Newton method. Nonlinear elimination is a nonlinear preconditioning technique based on the identification of variables and equations of \mathbf{F} (e.g. strong nonlinearities) that slow down the convergence of Newton method. These components are then eliminated through the solution of a local nonlinear problem at every step of an outer Newton. This elimination step provides a better initial guess for the outer iteration, so that a faster convergence is achieved [22, 41].

In light of the possible singularity of $\tilde{\mathbf{J}}$, we split the discretized variables $\tilde{\mathbf{x}}$ into $\tilde{\mathbf{x}} = (\mathbf{x}, t)$, and we aim to eliminate the variables \mathbf{x} to obtain a scalar nonlinear equation only for t . To do so, we partition (5.4) as

$$(5.11) \quad \tilde{\mathbf{F}} \begin{pmatrix} \mathbf{x} \\ t \end{pmatrix} = \begin{pmatrix} \mathbf{F}_1(\mathbf{x}, t) \\ F_2(\mathbf{x}, t) \end{pmatrix} = \begin{pmatrix} \mathbf{0} \\ 0 \end{pmatrix},$$

where $\mathbf{F}_1 = (\tilde{\mathbf{F}}_1(\mathbf{x}, t), \tilde{\mathbf{F}}_2(\mathbf{x}, t), \tilde{\mathbf{F}}_3(\mathbf{x}, t))$ and $F_2(\mathbf{x}, t) = \tilde{F}_4(\mathbf{x}, t)$. Similarly, $\tilde{\mathbf{J}}$ is partitioned into

$$\tilde{\mathbf{J}} = \begin{pmatrix} \mathbf{J}_{1,1} & \mathbf{J}_{1,2} \\ \mathbf{J}_{2,1} & J_{2,2} \end{pmatrix}$$

whose blocks have dimensions $\mathbf{J}_{1,1} \in \mathbb{R}^{(2N+1)N_h \times (2N+1)N_h}$, $\mathbf{J}_{1,2} \in \mathbb{R}^{(2N+1)N_h \times 1}$, $\mathbf{J}_{2,1} \in \mathbb{R}^{1 \times (2N+1)N_h}$, and $J_{2,2} \in \mathbb{R}$. Notice that $\mathbf{J}_{1,1}$ is always nonsingular, while $\mathbf{J}_{2,1}$, $\mathbf{J}_{1,2}$ and $J_{2,2}$ are identically zero if (5.10) is verified. Thus \mathbf{F}_1 allows us to define an implicit map $h : \mathbb{R} \rightarrow \mathbb{R}^{(2N+1)N_h}$, such that $\mathbf{F}_1(h(t), t) = \mathbf{0}$, so that the first set of nonlinear equations in (5.11) are satisfied. We are then left to solve the nonlinear scalar equation

$$(5.12) \quad F(t) = 0, \quad \text{where} \quad F(t) := F_2(h(t), t).$$

To do so using the Newton method, we need the derivative of $F(t)$ evaluated at $t = t^k$ which, using implicit differentiation, can be computed as

$$F'(t^k) = J_{2,2}(h(t^k), t^k) - \mathbf{J}_{2,1}(h(t^k), t^k) (\mathbf{J}_{1,1}(h(t^k), t^k))^{-1} \mathbf{J}_{1,2}(h(t^k), t^k).$$

The nonlinear preconditioned Newton method is described in Alg. 5.1, and consists in solving (5.12) with Newton method. However, to overcome the possible singularity of $J_{2,2}^k$, $\mathbf{J}_{1,2}^k$ and $\mathbf{J}_{2,1}^k$, we check at each iteration k if (5.10) is satisfied, and in the affirmative case we update \mathbf{x}^k by solving $\mathbf{F}_1(\mathbf{x}^{k+1}, t^k) = \mathbf{0}$ using Newton method, and update t^k by solving $F_2(\mathbf{x}^k, t^{k+1}) = 0$. Notice further, that each iteration of the backtracking line-search requires to solve $F_1(h(t), t) = 0$ using Newton method, thus additional linear systems with matrix $\mathbf{J}_{1,1}$ must be solved.

We report that we also tried to eliminate t by computing the map l such that $F_2(\mathbf{x}, l(\mathbf{x})) = 0$, while iterating on the variable \mathbf{x} . This has the advantage that l can be evaluated very cheaply, being a scalar equation. However, we needed many more

Algorithm 5.1 Nonlinear preconditioned Newton method to solve $\tilde{\mathbf{F}}(\tilde{\mathbf{x}}) = 0$.

Require: $t^0, \text{Tol} \in \mathbb{R}^+, \sigma, \rho \in (0, 1)$.

- 1: Compute $\mathbf{x}^0 = h(t^0)$ solving $\mathbf{F}_1(\mathbf{x}^0; t^0) = 0$ using the Newton method.
- 2: Set $k = 0$.
- 3: **while** $|F(t^k)| > \text{Tol}$ **do**
- 4: **if** (5.10) is satisfied **then**
- 5: Compute \mathbf{x}^{k+1} and t^{k+1} solving $\mathbf{F}(\mathbf{x}^{k+1}; t^k) = 0$ and $\tilde{F}_4(\mathbf{x}^k; t^{k+1}) = 0$.
- 6: **else**
- 7: Compute descend Newton's direction $d = -(F'(t^k))^{-1}F(t^k)$. Set $\gamma = 1$ and compute $\mathbf{x} = h(t^k + \gamma d)$ solving $\mathbf{F}_1(\mathbf{x}; t^k + d) = 0$.
- 8: **while** $|F(t^k + \gamma d)| - |F(t^k)| > -\sigma|F(t^k)|$ **do**
- 9: Set $\gamma = \rho\gamma$.
- 10: Compute $\mathbf{x} = h(t^k + \gamma d)$ solving $\mathbf{F}_1(\mathbf{x}; t^k + \gamma d) = 0$.
- 11: **end while**
- 12: Set $t^{k+1} = t^k + \gamma d, \mathbf{x}^{k+1} = \mathbf{x}, k = k + 1$.
- 13: **end if**
- 14: **end while**
- 15: **return** t^{k+1} and \mathbf{x}^{k+1} .

iterations both of the outer Newton method, and consequently of the inner linear solver. Thus, according to our experience, this second approach resulted less efficient and appealing.

5.2. Numerical experiments. In this section we report numerical tests to assess the performance of the preconditioned Newton algorithm to solve (5.5), and of the collective multigrid algorithm to invert the matrix $\mathbf{J}_{1,1}$. We consider the random PDE-constraint (3.4) with the random diffusion coefficient (3.5). Table 5 reports the number of outer and inner Newton iterations, and the average number of V-cycle iterations and of preconditioned GMRES iterations to solve the linear systems at each (inner/outer) Newton iterations. The outer Newton iteration is stopped when $|F(t^k)| \leq 10^{-6}$, the inner Newton method to compute $h(\cdot)$ is stopped when $\|\mathbf{F}_{1,1}(\mathbf{x}; t^k)\|_2 \leq 10^{-9}$, and the linear solvers are stopped when the (unpreconditioned) residual is smaller than 10^{-10} .

In Table 5, the number of outer Newton iterations is quite stable, while the number of inner Newton iterations varies between five and twenty iterations per outer iteration, essentially due to how difficult is to compute the nonlinear map $h(t)$ by solving $\mathbf{F}_1(\mathbf{x}; t^k) = 0$ in line (5), (8) and (11) of Alg. 5.1. The average number of inner linear solvers is quite stable as well. We emphasize that the top left blocks of $\mathbf{J}_{1,1}$ involve the matrices $C_i(\mathbf{y}_i^k, t^k)$ (see (5.8)) which contain a dense low-rank term if $g''_\varepsilon(Q_{\omega_i}^k) \neq 0$. Further, as $\varepsilon \rightarrow 0$, $g''_\varepsilon(\cdot)$ tends to a Dirac delta, so the dense term become dominant. Multigrid methods based on a pointwise relaxations are expected to be not very efficient for these matrices which may not be diagonally dominant. The standard V-cycle algorithm indeed struggles, however the Krylov acceleration performs much better as it handles these low-rank perturbation with smaller effort. We sometimes noticed that the GMRES residual stagnates after 20/30 iterations around $10^{-8}/10^{-9}$, due to a loss of orthogonality in the Krylov subspace. We allowed a maximum number of 80 GMRES iterations per linear system.

Figure 2 compares the two optimal controls obtained minimizing either $\mathbb{E}[Q(y_\omega)]$ or $\text{CVaR}_\lambda(Q(y_\omega))$, and the quantity of interests $Q(y_{\omega_j})$ for every sample discretization

TABLE 5

Number of preconditioned Newton iterations, and of V-cycle iterations and preconditioned GM-RES iterations (in brackets).

| | | | |
|------------|------------------|------------------|------------------|
| $N_h(N_L)$ | 81 (2) | 361 (3) | 1521 (4) |
| It. | 6-61-(33.4-18.2) | 7-74-(34.2-16.7) | 7-79-(30.1-20.7) |

$$\nu = 10^{-4}, \beta = 10^{-2}, N = 125, \sigma^2 = 0.5, L^2 = 0.5.$$

| | | | | |
|-----|--------------------|-------------------|--------------------|------------------|
| N | 8 | 27 | 64 | 125 |
| It. | 4-20-(19.34-13.16) | 8-188-(32.3-17.3) | 5-50-(27.85-15.73) | 7-85-(22.9-14.8) |

$$N_h = 961, \nu = 10^{-4}, \varepsilon = 10^{-2}, \lambda = 0.95, \sigma^2 = 1, L^2 = 0.5.$$

| | | | | |
|-----------|-------------|------------------|------------------|-------------------|
| λ | 0 | 0.5 | 0.95 | 0.99 |
| It. | 0-1-(21-15) | 6-80-(20.3-14.2) | 6-85-(22.9-14.8) | 7-124-(34.8-17.3) |

$$N_h = 961, \nu = 10^{-4}, \varepsilon = 10^{-2}, N = 125, \sigma^2 = 1, L^2 = 0.5.$$

| | | | | |
|---------------|-------------------|------------------|---------------------|------------------|
| ε | 10^{-1} | 10^{-2} | 10^{-3} | 10^{-4} |
| It. | 4-25-(21.12-14.8) | 2-13-(20.8-14.5) | 4-100-(27.79-15.98) | 1-27-(62.8-16.1) |

$$N_h = 961, \nu = 10^{-4}, \beta = 0.95, N = 125, \sigma^2 = 1, L^2 = 0.5.$$

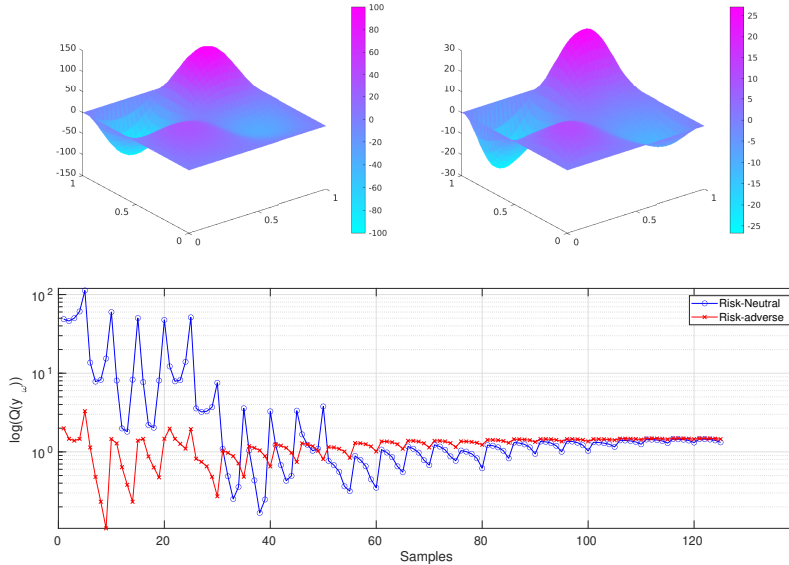


FIG. 2. Solution of the linear-quadratic OCP (top-left), solution of the smoothed risk-adverse OCP with $\lambda = 0.99$ (top-right), distribution of the quantity of interest $Q(y_\omega)$ (bottom-center).

at optimum. We remark that the risk-adverse control indeed minimizes the *risk* of having large values of $Q(y_\omega)$, at the price of leading to higher values of $Q(y_\omega)$ for most realizations. Notice that we used Gauss-Legendre nodes, so that not all realizations have the same weights. The more likely events are around the median, while the first 17 realizations count for around 1% of the discretized probability mass.

6. Conclusion. We have presented a multigrid method to solve the large saddle point linear systems that typically arise in full-space approaches to solve OCPUU.

We tested the algorithm as a iterative solver and as a preconditioner on three test cases: a linear-quadratic OCPUU, a nonsmooth OCPUU, and a risk-adverse nonlinear OCPUU. Overall, the multigrid method shows very good performances and robustness with respect to the several parameters of the problems considered.

7. Acknowledgements. Gabriele Ciaramella and Tommaso Vanzan are members of GNCS (Gruppo Nazionale per il Calcolo Scientifico) of INdAM.

REFERENCES

- [1] H. ANTIL, S. DOLGOV, AND A. ONWUNTA, *TTRISK: Tensor train decomposition algorithm for risk averse optimization*, arXiv preprint arXiv:2111.05180, (2021).
- [2] A. ASADPOURE, M. TOOTKABONI, AND J. K. GUEST, *Robust topology optimization of structures with uncertainties in stiffness - application to truss structures*, *Computers & Structures*, 89 (2011), pp. 1131–1141, <https://doi.org/https://doi.org/10.1016/j.compstruc.2010.11.004>, <https://www.sciencedirect.com/science/article/pii/S004579491000266X>. *Computational Fluid and Solid Mechanics* 2011.
- [3] I. BABUŠKA, F. NOBILE, AND R. TEMPONE, *A stochastic collocation method for elliptic partial differential equations with random input data*, *SIAM review*, 52 (2010), pp. 317–355.
- [4] A. BORZI, *Multigrid and sparse-grid schemes for elliptic control problems with random coefficients*, *Computing and visualization in science*, 13 (2010), pp. 153–160.
- [5] A. BORZI AND K. KUNISCH, *A multigrid scheme for elliptic constrained optimal control problems*, *Computational Optimization and Applications*, 31 (2005), pp. 309–333.
- [6] A. BORZI AND V. SCHULZ, *Multigrid methods for PDE optimization*, *SIAM review*, 51 (2009), pp. 361–395.
- [7] A. BORZI AND G. VON WINCKEL, *Multigrid methods and sparse-grid collocation techniques for parabolic optimal control problems with random coefficients*, *SIAM Journal on Scientific Computing*, 31 (2009), pp. 2172–2192.
- [8] E. CASAS, *A review on sparse solutions in optimal control of partial differential equations*, *SeMA Journal*, 74 (2017), pp. 319–344.
- [9] J. CHARRIER, *Strong and weak error estimates for elliptic partial differential equations with random coefficients*, *SIAM Journal on Numerical Analysis*, 50 (2012), pp. 216–246, <https://doi.org/10.1137/100800531>.
- [10] J. CHARRIER, R. SCHEICHL, AND A. L. TECKENTRUP, *Finite element error analysis of elliptic PDEs with random coefficients and its application to multilevel Monte Carlo methods*, *SIAM Journal on Numerical Analysis*, 51 (2013), pp. 322–352, <https://doi.org/10.1137/110853054>.
- [11] G. CIARAMELLA AND M. J. GANDER, *Iterative methods and preconditioners for systems of linear equations*, SIAM, 2022.
- [12] D. COHN, *Measure theory: second edition*, Birkhäuser Advanced Texts Basler Lehrbücher, Springer New York, 2013.
- [13] M. EIGEL, J. NEUMANN, R. SCHNEIDER, AND S. WOLF, *Risk averse stochastic structural topology optimization*, *Computer Methods in Applied Mechanics and Engineering*, 334 (2018), pp. 470–482.
- [14] I. EKELAND AND R. TEMAM, *Convex analysis and variational problems*, SIAM, 1999.
- [15] C. GEIERSBACH AND W. WOLLNER, *A stochastic gradient method with mesh refinement for PDE-constrained optimization under uncertainty*, *SIAM Journal on Scientific Computing*, 42 (2020), pp. A2750–A2772.
- [16] P. GUTH, V. KAARNIOJA, F. KUO, C. SCHILLINGS, AND I. SLOAN, *A Quasi-Monte Carlo method for optimal control under uncertainty*, *SIAM/ASA Journal on Uncertainty Quantification*, 9 (2021), pp. 354–383, <https://doi.org/10.1137/19M1294952>.
- [17] M. HINZE, R. PINNAU, M. ULBRICH, AND S. ULBRICH, *Optimization with PDE constraints*, vol. 23, Springer Science & Business Media, 2008.
- [18] D. P. KOURI, M. HEINKENSCHLOSS, D. RIDZAL, AND B. G. VAN BLOEMEN WAANDERS, *A trust-region algorithm with adaptive stochastic collocation for PDE optimization under uncertainty*, *SIAM Journal on Scientific Computing*, 35 (2013), pp. A1847–A1879.
- [19] D. P. KOURI AND A. SHAPIRO, *Optimization of PDEs with uncertain inputs*, in *Frontiers in PDE-Constrained Optimization*, Springer, 2018, pp. 41–81.
- [20] D. P. KOURI AND T. M. SUROWIEC, *Risk-averse PDE-constrained optimization using the conditional value-at-risk*, *SIAM Journal on Optimization*, 26 (2016), pp. 365–396, <https://doi.org/10.1137/140954556>.

- [21] D. P. KOURI AND T. M. SUROWIEC, *Existence and optimality conditions for risk-averse PDE-constrained optimization*, SIAM/ASA Journal on Uncertainty Quantification, 6 (2018), pp. 787–815.
- [22] P. J. LANZKRON, D. J. ROSE, AND J. T. WILKES, *An analysis of approximate nonlinear elimination*, SIAM Journal on Scientific Computing, 17 (1996), pp. 538–559.
- [23] C. LI AND G. STADLER, *Sparse solutions in optimal control of PDEs with uncertain parameters: The linear case*, SIAM Journal on Control and Optimization, 57 (2019), pp. 633–658.
- [24] J. LIONS, *Optimal control of systems governed by partial differential equations*, Die Grundlehren der mathematischen Wissenschaften in Einzeldarstellungen, Springer-Verlag, 1971.
- [25] G. J. LORD, C. E. POWELL, AND T. SHARDLOW, *An introduction to computational stochastic PDEs*, Cambridge Texts in Applied Mathematics, Cambridge University Press, 2014.
- [26] M. MARKOWSKI, *Efficient Solution of smoothed risk-adverse PDE-constrained optimization problems*, PhD thesis, Rice University, 2022.
- [27] J. MARTÍNEZ AND L. QI, *Inexact newton methods for solving nonsmooth equations*, Journal of Computational and Applied Mathematics, 60 (1995), pp. 127–145.
- [28] J. MARTÍNEZ-FRUTOS AND F. ESPARZA, *Optimal control of PDEs under uncertainty: an introduction with application to optimal shape design of structures*, Springer, 2018.
- [29] F. NOBILE AND T. VANZAN, *Preconditioners for robust optimal control problems under uncertainty*, accepted in Numerical linear algebra with applications.
- [30] F. NOBILE AND T. VANZAN, *A combination technique for optimal control problems constrained by random PDEs*, arXiv preprint arXiv:2211.00499, (2022).
- [31] J. W. PEARSON AND A. WATHEN, *A new approximation of the Schur complement in preconditioners for PDE-constrained optimization*, Numerical Linear Algebra with Applications, 19 (2012), pp. 816–829.
- [32] T. REES, H. S. DOLLAR, AND A. WATHEN, *Optimal solvers for PDE-constrained optimization*, SIAM Journal on Scientific Computing, 32 (2010), pp. 271–298.
- [33] R. T. ROCKAFELLAR, S. URYASEV, ET AL., *Optimization of conditional value-at-risk*, Journal of risk, 2 (2000), pp. 21–42.
- [34] E. ROSSEEL AND G. N. WELLS, *Optimal control with stochastic PDE constraints and uncertain controls*, Computer Methods in Applied Mechanics and Engineering, 213 (2012), pp. 152–167.
- [35] A. SHAPIRO, D. DENTCHEVA, AND A. RUSZCZYŃSKI, *Lectures on stochastic programming: modeling and theory*, SIAM, 2014.
- [36] G. STADLER, *Errata: Elliptic optimal control problems with l^1 -control cost and applications for the placement of control devices*. 2008, <https://cims.nyu.edu/~stadler/publications/index.html>.
- [37] G. STADLER, *Elliptic optimal control problems with l^1 -control cost and applications for the placement of control devices*, Computational Optimization and Applications, 44 (2009), pp. 159–181.
- [38] S. TAKACS AND W. ZULEHNER, *Convergence analysis of multigrid methods with collective point smoothers for optimal control problems*, Computing and Visualization in Science, 14 (2011), pp. 131–141.
- [39] F. TRÖLTZSCH, *Optimal control of partial differential equations: theory, methods, and applications*, Graduate studies in mathematics, American Mathematical Society, 2010.
- [40] M. ULBRICH, *Semismooth Newton Methods for Variational Inequalities and Constrained Optimization Problems in Function Spaces*, Society for Industrial and Applied Mathematics, 2011.
- [41] H. YANG, F.-N. HWANG, AND X.-C. CAI, *Nonlinear preconditioning techniques for full-space lagrange–newton solution of PDE-constrained optimization problems*, SIAM Journal on Scientific Computing, 38 (2016), pp. A2756–A2778, <https://doi.org/10.1137/15M104075X>.

MOX Technical Reports, last issues

Dipartimento di Matematica
Politecnico di Milano, Via Bonardi 9 - 20133 Milano (Italy)

- 17/2023** Savin, M.S.; Cavinato, L.; Costa, G.; Fiz, F.; Torzilli, G.; Vigano', L.; Ieva, F.
Distant supervision for imaging-based cancer sub-typing in Intrahepatic Cholangiocarcinoma
- 19/2023** Marcinno', F.; Vergara, C.; Giovannacci, L.; Quarteroni, A.; Prouse, G.
Computational fluid-structure interaction analysis of the end-to-side radio-cephalic arteriovenous fistula
- 15/2023** Ragni, A.; Masci, C.; Ieva, F.; Paganoni, A. M.
Clustering Hierarchies via a Semi-Parametric Generalized Linear Mixed Model: a statistical significance-based approach
- Bertoletti, A.; Cannistrà, M.; Diaz Lema, M.; Masci, C.; Mergoni, A.; Rossi, L.; Soncin, M.
The Determinants of Mathematics Achievement: A Gender Perspective Using Multilevel Random Forest
- 13/2023** Masci, C.; Cannistrà, M.; Mussida, P.
Modelling time-to-dropout via Shared Frailty Cox Models. A trade-off between accurate and early predictions
- 11/2023** Gatti, F.; Perotto, S.; de Falco, C.; Formaggia, L.
A positivity-preserving well-balanced numerical scheme for the simulation of fast landslides with efficient time stepping
- 10/2023** Corti, M.; Antonietti, P.F.; Bonizzoni, F.; Dede', L., Quarteroni, A.
Discontinuous Galerkin Methods for Fisher-Kolmogorov Equation with Application to Alpha-Synuclein Spreading in Parkinson's Disease
- 09/2023** Buchwald, S.; Ciaramella, G.; Salomon, J.
Gauss-Newton oriented greedy algorithms for the reconstruction of operators in nonlinear dynamics
- 08/2023** Bonizzoni, F.; Hu, K.; Kanschat, G.; Sap, D.
Discrete tensor product BGG sequences: splines and finite elements
- 06/2023** Artoni, A.; Antonietti, P. F.; Mazzieri, I.; Parolini, N.; Rocchi, D.
A segregated finite volume - spectral element method for aeroacoustic problems